Atomization Characteristics and Prediction Accuracy of LISA-DDB Model for Gasoline Direct Injection Spray

Sung Wook Park, Hyung Jun Kim
Graduate School of Hanyang University,
17 Haengdang-dong, Sungdong-gu, Seoul 133-791, Korea
Ki Hyung Lee, Chang Sik Lee*
Department of Mechanical Engineering, Hanyang University,
17 Haengdang-dong, Sungdong-gu, Seoul 133-791, Korea

In this paper, the spray atomization characteristics of a gasoline direct-injection injector were investigated experimentally and numerically. To visualize the developing spray process, a laser sheet method with a Nd:YAG laser was utilized. The microscopic atomization characteristics such as the droplet size and velocity distribution were also obtained by using a phase Doppler particle analyzer system at the 5 MPa of injection pressure. With the experiments, the calculations of spray atomization were conducted by using the KIVA code with the LISA-DDB breakup model. Based on the agreement with the experimental results, the prediction accuracy of LISA-DDB breakup model was investigated in terms of the spray shapes, spray tip penetration, SMD distribution, and axial mean velocity. The results of this study provides the macroscopic and microscopic characteristics of the spray atomization, and prediction accuracy of the LISA-DDB model.

Key Words: Hybrid Breakup Model, Atomization Characteristics, GDI (Gasoline Direct Injection), KIVA-3 Code

Nomenclature

a	: Ellipse major axis
C_D	: Drag coefficient
C_{DS}	: Drag coefficient of the sphere
d_o	: Orifice diameter
d_D	: Diameter after breakup
d_L	: Diameter of the ligament
h_0	: Sheet thickness
K	: Density ratio of liquid-gas
K_L	: Most unstable wave number of LISA model
k_v	: Velocity coefficient
L_b	: Breakup length
$\dot{m}$	: Mass flow rate
N	: Viscosity ratio of liquid-gas
Δp	: Injection pressure
r	: Initial droplet spherical radius
Re	: Reynolds number
U	: Total sheet velocity
u	: Axial component of the velocity at the nozzle exit
We	: Weber number
y	: Magnitude of drop deformation
η_0	: Initial amplitude
η_b	: Critical amplitude
ρ	: Density
Ω	: Maximum growth rate

Subscripts

g	: Gas properties
l	: Liquid properties

Abbrerations

GDI : Gasoline direct injection

* Corresponding Author,
E-mail: cslee@hanyang.ac.kr
TEL: +82-2-2290-0427; **FAX**: +82-2-2281-5286
Department of Mechanical Engineering, Hanyang University, 17 Haengdang-dong, Sungdong-gu, Seoul 133-791, Korea. (Manuscript **Received** September 8, 2003; **Revised** February 10, 2004)

PDPA: Phase Doppler particle analyzer
SMD : Santer mean diameter
UBH : Unburned hydrocarbon

1. Introduction

The advantages of the gasoline direct-injection (GDI) engine over the port-injection engine are the improved fuel economy, reduced unburned hydrocarbons (UBH) and CO_2 emissions, and more precise air-fuel ratio control. In spite of the benefit of GDI combustion, there are many problems such as the complete evaporation of the fuel, the increase of UBH, and the difficulties in maintaining of stratification in the combustion chamber. In order to apply gasoline direct-injection system to the engine, the fuel injector of a GDI engine must be designed to produce well-atomized spray at very short duration in comparison to the conventional gasoline engine. To solve these problems, many researchers have investigated spray behavior and atomization characteristics of high-pressure gasoline swirl injector for a direct injection gasoline engine.

Recently, a comprehensive overview on the mixture formation and combustion control in a spark-ignited direct-injection gasoline engine was reported by Zhao et al.(1995). Michael et al.(1998) investigated the early spray development of three different injectors at various injection pressures for the optical engine with PLIF system. The results of this work show the spray development processes and the range of cone angle and penetration depth in an engine. Miyajima et al.(2003) have studied on the optimal DI injector that reduces fuel spray impingement and improves the combustion stability based on the fuel spray pattern. In their study, in order to improve stratified-charge combustion system in the SI engine, flat-shape spray pattern was developed. Also, Lee et al.(2001) have investigated the effect of injection pressure on the atomization characteristics of the injection spray by using spray visualization system and droplet measuring system. They reported that the mean droplet size is decreased and the velocity of droplet becomes faster with the increase of injection pressure. And York et al.(1953) and Fraser et al.(1962) have studied the disintegration of liquid sheet such as flat, conical, and fan sheet on the pressure swirl nozzle.

Also many researchers have suggested breakup models based on the various breakup mechanisms at different operation conditions. Schmidt et al. (1999) proposed the hybrid model that is composed of LISA model and TAB model (O'Rourke et al. 1987) for the primary breakup and secondary breakup, respectively. The DDB model that is based on the dynamics of the motion of the center of mass of the half-drop is proposed by Ibrahim et al.(1993) to predict drop breakup of high-speed diesel spray. Many other studies (Park and Lee, 2003; Park et al., 2003) on the spray atomization characteristics were performed experimentally and numerically.

The results of the previous researches provide detail characteristics of fuel injector spray and breakup mechanism of the spray. However, due to experimental difficulty and complicated phenomena of spray development, detailed information about the spray breakup and characteristics of the direct-injection spray is still needed.

The objective of this work is to investigate the macroscopic and microscopic characteristics of gasoline injector for GDI engine by numerical approach applying the LISA-DDB hybrid breakup model and experimental method. The global spray behaviors such as spray tip penetration and spray shape of fuel injector are visualized by the laser light source and a CCD camera, and the atomization characteristics such as spray droplet size and velocity distribution of the gasoline direct injector are measured by using phase Doppler particle analyzer system. The LISA-DDB hybrid breakup model is used to obtain the results of the numerical calculation. Based on the results of the calculation, the numerical results of the hybrid models are compared with the experimental results such as spray shape, local SMD, axial mean velocity, and the distribution of the droplet breakup.

2. LISA-DDB Model

2.1 Concept of LISA-DDB breakup model

KIVA-3 code with LISA-DDB breakup model is used to calculate the atomization process of the injected spray. Figure 1 shows a concept of the LISA-DDB breakup model. After injection, the primary breakup model governs the breakup and it is assumed that the droplets do not undergo breakup, collision, and drag until the droplet reaches a distance from the injector greater than the breakup length of the LISA model. At the breakup length, the LISA model disintegrates the droplets. After the primary breakup, the droplets are further disintegrated by the DDB model.

2.2 Primary breakup model (LISA model)

For the primary breakup, Schmidt et al.(1999) proposed Linearized Instability Sheet Atomization (LISA) model. It is assumed that the injector exit velocity profile is uniform and the total velocity U is related to the injection pressure Δp.

$$U=k_v\sqrt{\frac{2\Delta p}{\rho_l}} \tag{1}$$

where the velocity coefficient k_v is given by the following equation (Schmidt et al., 1999).

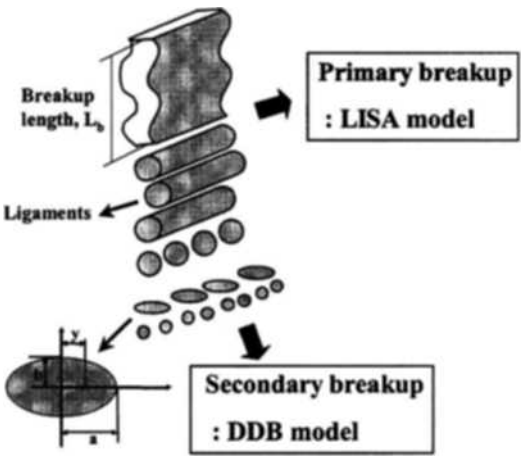

Fig. 1 Concept of LISA-DDB breakup model

$$k_v=\max\left[0.7,\ \frac{4\dot{m}}{\pi d_0^2\rho_l\cos\theta\sqrt{\frac{\rho_l}{2\Delta p}}}\right] \tag{2}$$

and the axial component of the velocity at the nozzle exit, calculated from

$$u=U\cos\theta \tag{3}$$

Also, the initial sheet thickness h_0 is related to the mass flow rate $\dot{m}$ and the axial component of velocity u at the injector exit. The mass flow rate $\dot{m}$ is given by

$$\dot{m}=\pi\rho_l u h_0(d_0-h_0) \tag{4}$$

The LISA model assumed that the drag on the sheet and the displacement of air by sheet volume is neglected because the liquid sheet does not directly relate with the gas phase. Therefore, the droplet undergoes no breakup, no collision, and no drag until it reaches to the breakup length L_b, which is given by (Schmidt et al., 1999)

$$L_b=\frac{U}{\Omega}\ln\left(\frac{\eta_b}{\eta_0}\right) \tag{5}$$

where, the quantity $\ln(\eta_b/\eta_o)$ is proposed the value 12 by Dombrowski et al. (1963). And the new diameter d_D after breakup at the breakup length is given by

$$d_D^3=\frac{3\pi d_L^2}{K_L} \tag{6}$$

where d_L is the diameter of the ligament and K_L is the most unstable wave number.

2.3 Secondary breakup model (DDB model)

The drop deformation and breakup(DDB) model is based on the conservation of energy for a distorting droplet and proposed by Ibrahim et al.(1993). The model is assumed that the droplet is distorted by pure extension flow.

In the DDB model, the governing equation of the model is given by

$$K\frac{d^2y}{dt^2}+\frac{4N}{\mathrm{Re}}\frac{1}{y^2}\frac{dy}{dt}+\frac{27\pi^2}{16We}Y[1-2(cy)^{-6}]=\frac{3}{8} \tag{7}$$

In this equation, K is the liquid-gas of density ratio, N is the liquid-gas of viscosity ratio and $c=3\pi/4$. The value of y is calculated with a

fourth-order Runge-Kutta method and the droplet breaks up when the ratio of the major semi-axis of the ellipsoidal cross section of the oblate spheroid a to the initial droplet spherical radius r is greater than the critical condition. Also, the critical condition of the drop breakup is given by the following equation :

$$\frac{a}{r}=\frac{We}{6\pi} \tag{8}$$

In the DDB model, the drop drag coefficient is related to a function of the droplet Reynolds number and the equation is given by (Liu et al., 1993)

$$C_{DS}=\frac{24}{Re_l}\left(1+\frac{1}{6}Re_l^{\frac{2}{3}}\right) \quad (Re_l \leq 1000) \tag{9}$$

$$C_{DS}=0.424 \quad (Re_l \geq 1000) \tag{10}$$

where, C_{DS} is the drag coefficient of the sphere and the drag coefficient C_D with the consideration of droplet is given by

$$C_D=C_{DS}(1+2.632y) \tag{11}$$

where, the drop drag coefficient based on the magnitude of the droplet deformation in eq. (11) is calculated using (Hwang et al., 1996)

$$y=\text{mim}\left\{1, \left(\frac{a}{r}-1\right)\right\} \tag{12}$$

3. Experimental Apparatus and Procedures

Figure 2 shows the experimental apparatus of the visualization system with the laser sheet method for to visualize the spray shape and process of spray development and phase Doppler particle analyzer (PDPA) system for the measurement of the SMD distribution and axial mean velocity of droplet. The spray visualization system is composed of the laser light source (Nd : YAG), a cylindrical lens and a CCD camera with an image acquisition system. Also, the analyzer system consists of 5 W Ar-ion laser, optical receiver, transmitter, and signal processor. The injection timing and injection duration are controlled by the computer system through the delay generator. And frozen images of a spray are captured onto the image grabber of the CCD camera with a 50 mm lens and the measurement points are selected at an interval of 2 mm in the radial direction and 5 mm in the axial direction for investigation of the droplet size and axial mean velocity of spray as illustrated in Fig. 3. Table 1 shows the specifications of the particle analyzing system and visualization system. In this experiment, 10,000 or more sampling data are obtained at each measurement points of PDPA system and the average value is calculated.

In this experiment a high-pressure swirl injector with 1.0 mm of nozzle hole diameter was used. After the fuel is fed into a swirl chamber through tangential ports, the air-cored vortex is created by a high angular velocity. And the fuel sprays through the outlet from the swirl chamber are emerged from the atomizer in the form

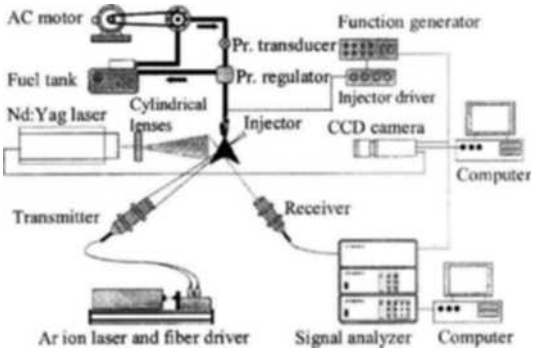

Fig. 2 Schematic diagram of PDPA system and spray visualization system

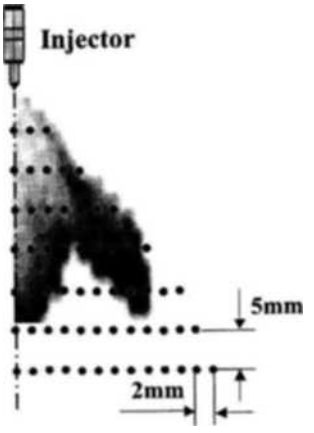

Fig. 3 Location of measurement points

of a hollow conical sheet by the rotating flows with axial and radial forces. The high-pressure injection system is composed of a fuel feed pump, a high-pressure pump, and a pressure-regulating system. The fuel is pressurized by the high-pressure pump driven by a 0.75 kW AC motor, and the signal controller controls injection timing. The test fuel used in this work is Stoddard solvent because its properties are very similar to those of gasoline and it has a low volatility. Tables 2 and 3 show the comparison of properties between iso-octane and Stoddard-solvent and the test conditions.

Table 1 Specifications of the PDPA and spray visualization system

PDPA system	
Laser power	1.5 W Ar-ion
Transmitting optics	85 mm Fiber Flow (2D)
	60 mm Fiber Flow (1D)
Focal lengths :	Transmitting : 310 mm
	Receiving : 310 mm
Scattering angle :	40
Polarization :	Parallel
Visualization system	
Laser source	Nd : YAG (Q-switched)
Wave length	532 nm
Laser power	270 mJ (max)
Beam thickness	~1.0 mm

Table 2 Comparison of properties between iso-octane and Stoddard-Solvent

Properties	Iso-Octane	Stoddard-Solvent
Specific weight [N/m^3]	0.692	0.772
Density [kg/m^3]	690	770
Viscosity [$kg/ms \times 10^5$]	1.253	1.210
Surface tension [mN/m]	2.653	2.901

Table 3 Test conditions

Injection pressure	5 MPa
Injection duration	7 ms
Injected mass	35.83 mg/cycle
Initial calculation time interval	20 μs
Grid size	1 mm × 1 mm

4. Results and Discussions

4.1 Development of global spray

Figure 4 shows the comparison between the experimental shapes of the spray from the spray visualization system and the numerical results of LISA-DDB model at 5 MPa of injection pressure from 1 msec to 7 msec after the start of injection (SOI). Comparing the experimental spray shape with the calculated one, the calculated images show good agreement with the experimental results. It is shown that test injector produces a typical fuel spray of hollow cone injector accompanying with the vortex on the spray surface. At the early stage of injection duration, the pre-spray is injected toward to the direction of axis of the injector and the droplets of the pre-spray are disintegrated by the effect of surrounding gas. By the effect of high drag force, the axial velocity of the disintegrated droplets of the pre-spray are slower than those of the main-spray and the pre-spray is merged into the main-spray finally. In the case of the main-spray, the velocity of gas increased due to droplets with high velocity and droplets cause the gas flow to circulate through the spray. While droplets move to downstream from the injector tip, the droplets disintegrate into small ones. The gas vortex has a tendency to carry the small droplets upward and the vortex cloud is formed as illustrated in the shape at 3 ms after start of injection as shown in Fig. 4. The outward circular vortex is created by the relative velocity between the ambient gas and the fuel spray is more clear and large as the elapsed time after start of injection increases.

In the calculated results of the LISA-DDB model, a stronger phenomenon of the vortex flow is observed. It can be estimated that the breakup criterion of DDB model is good for predicting the atomization of gasoline direct injection spray and it reduces the radius of droplet at the proper timing. The droplets that have low momentum due to droplet breakup and drag force are dispersed more rapidly. Concerning the calculated

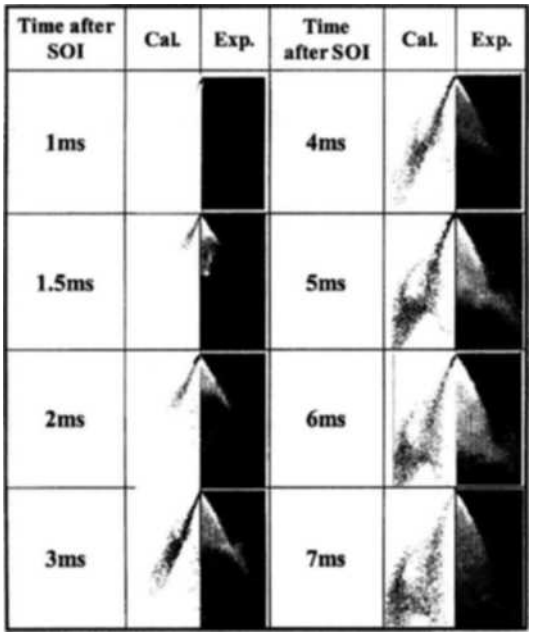

Fig. 4 Spray developing process

shapes of spray, the vortex of cloud is observed at the edge of spray because the dispersed droplets that have small momentum go upward due to the circulation of the surrounding gas at the edge of spray.

Figure 5 shows the comparison of experimental and calculated spray tip penetrations at the 5 MPa of the injection pressure. As indicated in this figure, the experimental and numerical results show similar tendency in the both cases of pre-spray and main-spray. However the calculated results are somewhat longer than the experimental results in the pre-spray. Probably the spray width of the experiment is wider than the calculated results at the pre-spray. In the case of the main-spray, the experimental results are longer than the calculated results at the 2~4 ms after start of injection because the predicted diameter of droplet is larger than experimental result at the early stage of injection. In the case of the pre-spray, it is founded that the LISA-DDB model predicts much shorter spray tip penetration than the experiments in the far field of the injected spray, because the LISA-DDB model overestimates the atomization of pre-spray.

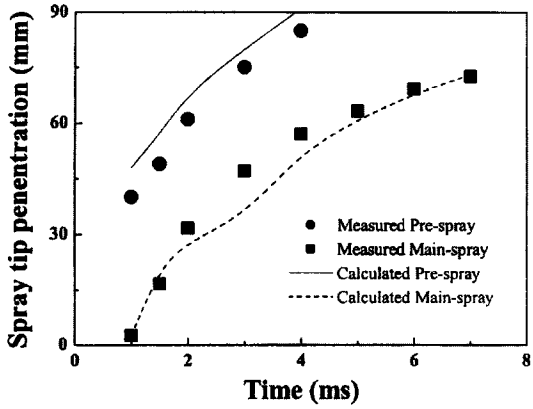

Fig. 5 Comparison with experimental and numerical results on the spray tip penetration

4.2 Atomization characteristics

Fig. 6 shows the comparison of experimental and calculated SMD contour of the spray from the phase Doppler particle analyzer system and KIVA code with LISA-DDB model. According to the predicted results of SMD contours by the LISA-DDB model, the SMD contours is similar with the experimental results with the exception of cylindrical image of the fuel spray. It is revealed that the experimental results of mean diameter distributions are larger than those of calculated results because the floating droplets are captured and involved the experimental images. On the whole, it is shown that the experimental and calculated results are similar tendency of SMD distribution.

Figure 7 shows the comparison between experimental and numerical results of radial SMD distributions from 20 mm to 60 mm downstream from the injector tip with the 20 mm intervals. As illustrated in the SMD distribution, the numerical results show comparatively good agreement with the experimental results. The comparison of SMD distribution at 20 mm of axial distance shows that the SMD value is ranged in the distribution of 15~25 mm. But the value of SMD increases due to the effect of pre-spray at the range of 0~5 mm of radial distance in Fig. 7(b). Also, it is shown that the SMD distribution at the range from 20 mm to 30 mm of radial distance show large value of SMD because the main

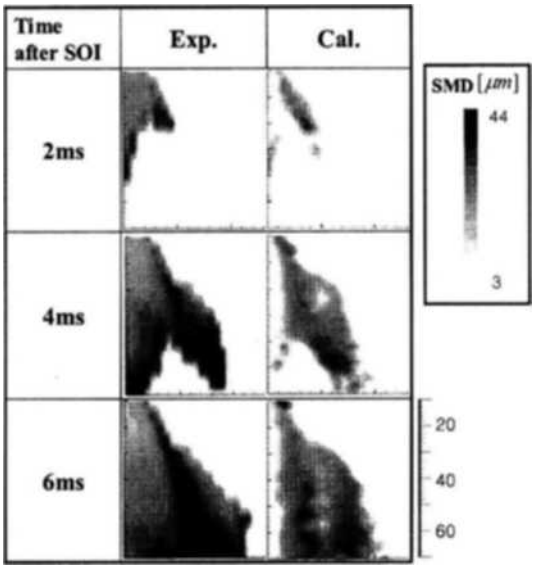

Fig. 6 Comparison between experimental and calculated SMD contours

stream of spray passes through this region. But, after injection the measured local SMD distributions at 60 mm downstream from the injector tip increases by the effect of the coalescence. As shown in Fig. 7, it is found that the SMD distributions of LISA-DDB model are similar to the measured SMD. From this trend, it can be estimated that the breakup criterion of DDB model that is closely related to Weber number is proper to calculate the atomization of high-speed gasoline direct spray.

Figure 8 shows the experimental and numerical results of axial mean velocity from 20 mm to 60 mm downstream from the injector tip at 5 MPa of injection pressure. The measured and calculated axial mean velocities in the case of (a) have maximum value at 8~10 mm of radial distance from the axis of the injector, because the main stream passes through this region. However the axial mean velocity of outward radial distance of 10 mm rapidly decreases due to the effect of surrounding gas. In the case of the Figs. 8(b) and (c) the measured and calculated axial mean velocity has peak value at the radial distance within 5 mm from the center. After the maximum value of the axial mean velocity shows a slight decline. Maybe the mean velocity of the droplets

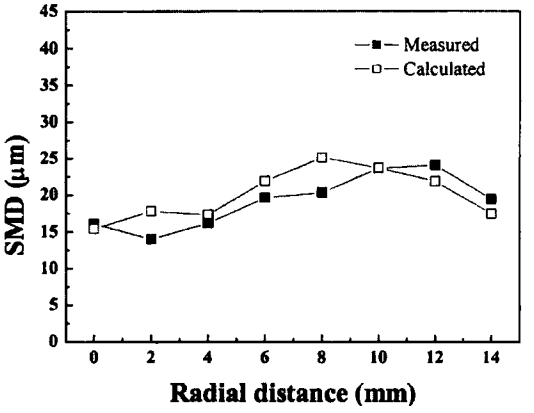

(a) Axial distance=20 mm

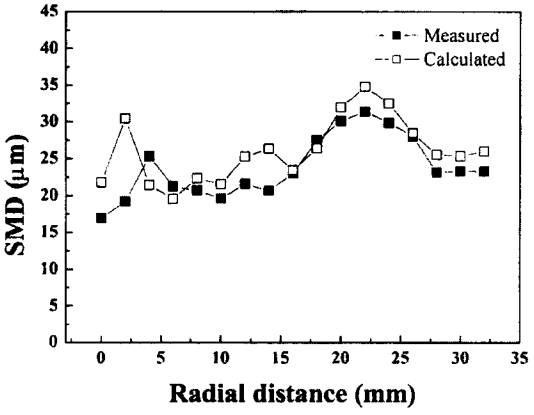

(b) Axial distance=40 mm

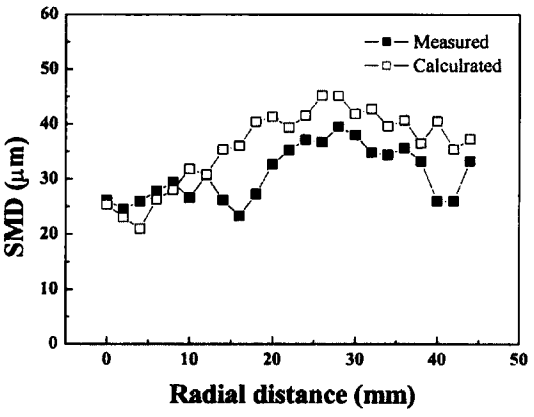

(c) Axial distance=60 mm

Fig. 7 Patterns of SMD distributions according to radial distance

becomes smaller as they go downstream, because the droplet velocity is decreased by the drag of surroundings gas and the loss of the momentum.

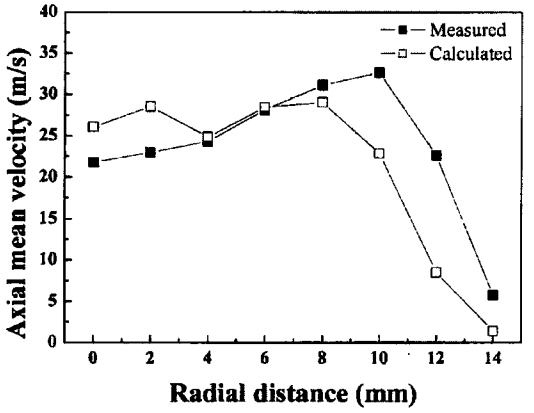

(a) Axial distance=20 mm

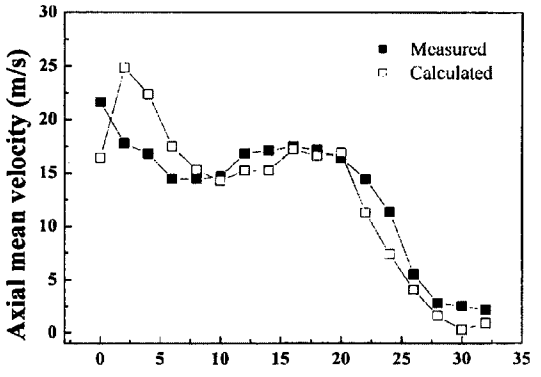

(b) Axial distance=40 mm

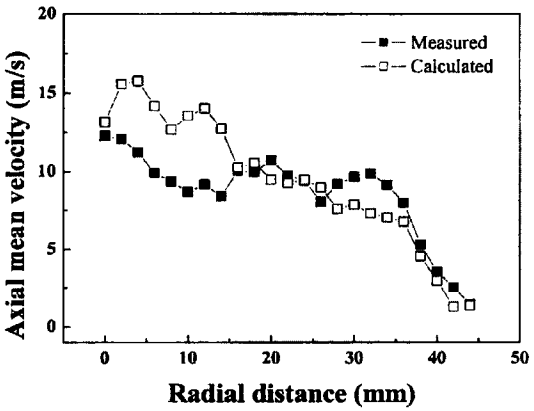

(c) Axial distance=60 mm

Fig. 8 Patterns of axial mean velocity distributions

To analyze the breakup characteristics of the LISA-DDB model, the spatial distribution of breakup is investigated at 5 MPa of injection pressure as illustrated in Fig. 9. In this figure, the percentage of breakup is calculated by dividing

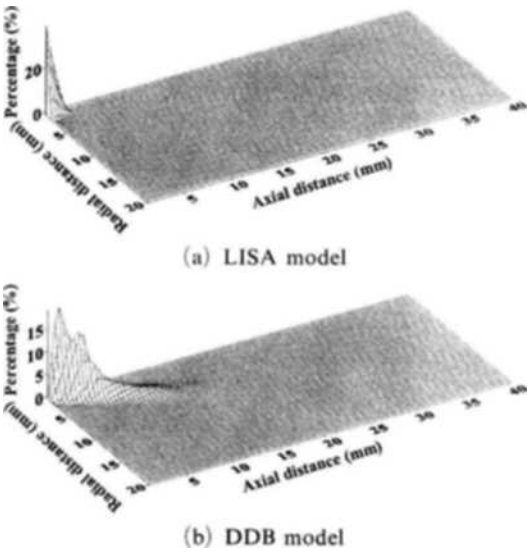

Fig. 9 Spatial distributions of breakup

the count of droplet breakup in a specific area of 1.0 mm×1.0 mm by the count of breakup in the whole area. The breakups of the LISA model is concentrated in the vicinity of the injector tip and it can be conducted that the atomization of the liquid sheet is almost finished at 2 mm upstream from the injector tip. On the other hand, the secondary breakup with the DDB model occurs from near the injector to the downstream and is distributed more widely in comparison to the primary breakup. After the primary breakup is occurred, the droplets have high velocity and momentum, that is, they take high value of Weber number. In the case of the DDB model, the breakup criterion is changed by Weber number in the eq. (8) and many breakups happen at the early stage of the secondary breakup.

Figure 10 illustrates the prediction error of the LISA-DDB models on the spray tip penetration, SMD distribution, and axial mean velocity. The prediction error is obtained from the following equation :

$$\varepsilon(\%) = \frac{\sum \frac{|V_C - V_M|}{V_M}}{N} \times 100 \qquad (13)$$

where N is the number at the sampling points. V_C and V_M indicate the calculated and measured value, respectively. As illustrated in Fig. 10, the

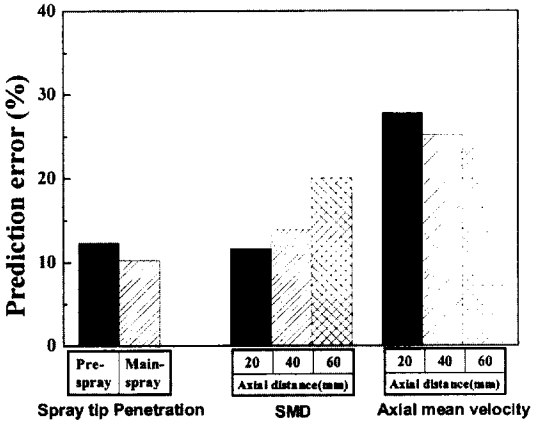

Fig. 10 Prediction error of LISA-DDB model

prediction error of the LISA-DDB model on spray tip penetration is relatively good in the both cases of the pre-spray and the main-spray. Concerning to the radial SMD distribution, it shows good accuracy at 20 mm of axial distance. However, the prediction error is increased with the increase of axial distance. On the other hand it is revealed that the prediction accuracy on axial mean velocity is inferior to those of spray tip penetration and SMD distribution.

5. Conclusions

This study conducts to analyze the macroscopic and microscopic characteristics of the gasoline direct-injection spray and investigates the prediction accuracy of LISA-DDB model in terms of developing spray process, spray tip penetration, SMD distribution, and axial mean velocity.

The conclusions of this study are summarized as follows:

(1) The spray shape of the LISA-DDB model shows good agreement with the experimental shape. The outward circular vortex that is created by the relative velocity between the ambient gas and the fuel spray is more clear and large with the increase of injection duration.

(2) The experimental and numerical results of spray tip penetration show similar tendency at the pre-spray and the main-spray. However it is found that the pre-spray of the LISA-DDB model predicts somewhat shorter spray tip penetration than the measured results in the far field, because the LISA-DDB model overestimates the atomization of pre-spray.

(3) It is shown that the calculated results of SMD from the LISA-DDB model show similar tendency with the experimental results. The measured and calculated results of axial mean velocity have the maximum value at the radial distance of 8~10 mm but the axial mean velocity of outward radial distance of 10 mm is decreased rapidly by the effect of surroundings gas.

(4) In the case of the spatial distribution of breakup on the LISA-DDB model, the breakup of the LISA model is concentrated on the injector tip but the secondary breakup using the DDB model occurs from near the injector to the downstream.

(5) The prediction error rate of the LISA-DDB model on spray tip penetration is relatively good at both the pre-spray and the main-spray. In the case of the radial SMD distribution, the prediction error rate is increased with the increase of axial distance.

Acknowledgment

This work was supported by Korea Research Foundation Grant (KRF-2002-042-D00025).

References

Dombrowski, N. and Johns, W. R., 1963, "The Aerodynamic Instability and Disintegration of Viscous Liquid Sheets," *Chem. Eng. Sci.*, Vol. 18, pp. 203~214.

Fraser, R. P., Eisenklam, P., Dombrowski, N. and Hasson, D., 1962, "Drop Formation from Rapidly Moving Sheets," *AIChE J.*, Vol. 8, No. 5, pp. 672~680.

Hwang, S. S., Liu, Z. and Reitz, R. D., 1996, "Breakup Mechanisms and Drag Coefficients of High-speed Vaporizing Liquid Drops," *Atomization and Sprays*, Vol. 6, pp. 353~376.

Ibrahim, E. A., Yang, H, Q. and Prezkwas, A. J., 1993, "Modeling of Spray Droplets Deformation and Breakup," *AIAA J. Propulsion and Power*, Vol. 9, No. 5, pp. 652~654.

Lee, C. S., Lee, K. H., Chon, M. S. and Kim, D. S., 2001, "Spray Structure and Characteristics of High-pressure Gasoline Injectors for Direct-injection Engine Applications," *Atomization and Sprays*, Vol. 11, pp. 35~48.

Liu, A. B., Mather, D. and Reitz, R. D., 1993, "Effect of Drop Drag and Breakup on Fuel Spray," SAE paper 930072.

Michael, H. S., Brad, A. V. and Hochgreb, S., 1998, "Early Spray Development in Gasoline Direct-Injected, Spark-Ignition Engines," SAE paper 980160.

Miyajima, A., Okamoto, Y., Kadomuki, Y., Kashiwaya, M., Kub, H. and Fujii, H., 2003, "Experimental Characterization of Flat-Spray Injector in Gasoline Direct Injection Engines," SAE paper 2003-01-0061.

O'Rourke, P. J. and Amsden, A. A., 1987, "The Tab Method for Numerical Calculation of Spray Droplet Breakup," SAE paper 872089.

Park, S. W. and Lee, C. S., 2003, "Macroscopic structure and atomization characteristics of high-speed diesel spray," *International Journal of Automotive Technology*, Vol. 4, pp. 157~164.

Park, S. W., Kim, H. J. and Lee, C. S., 2003, "Numerical and Experimental Analysis of Spray Atomization Characteristics of a GDI injector," *KSME International Journal*, Vol. 17, pp. 449~456.

Schmidt, D. P., Nouar, I., Senecal, P. K., Rutland, C. J., Martin, J. K., Reitz, R. D. and Hoffman, J. A., 1999, "Pressure-Swirl Atomization in the Near Field," SAE paper 1999-01-0496.

York, J. L., Stubbs, H. F. and Tek, M. R., Trans., 1953, "The Mechanism of Disintegration of Liquid Sheet," *Trans. ASME*, Vol. 75, pp. 1279~1286.

Zhao, F. Q., Lai, M. C. and Harrington, D. L., 1995, "The Spray Characteristics of Automotive Port Fuel Injection-A critical review," SAE paper 950506.